Journal of Alloys and Compounds 480 (2009) 885–888

Contents lists available at ScienceDirect

Journal of Alloys and Compounds

journal homepage: www.elsevier.com/locate/jallcom

Corrosion behavior of G-X CrNiMoNb 18-10 austenitic stainless steel in acidic solutions

S. Zor[b,*], M. Soncu[a], L. Çapan[a,*]

[a] Kocaeli Universty, Engineering Faculty, Department of Machine Eng., 41380, Kocaeli, Turkey
[b] Kocaeli University Science Art Faculty, Department of Chemistry, 41380, Kocaeli, Turkey

ARTICLE INFO

Article history:
Received 23 September 2008
Received in revised form 18 February 2009
Accepted 19 February 2009
Available online 4 March 2009

Keywords:
Austenitic stainless steel
Corrosion
Acidic solutions

ABSTRACT

The corrosion behaviors of G-X CrNiMoNb 18-10 austenitic stainless steel in (0.1, 1, 2 and 3 M) HCl, H_2SO_4, and H_2SO_4 + HCl (1:1) acidic solutions was investigated by the potentiodynamic polarization method and the weight loss method. Furthermore, the corrosion strength of austenitic stainless steel that exposed to acidic solutions for a specific duration of time was determined by hardness measurements. The chrome and other elements (Ni, Mo, etc.) contents of G-X CrNiMoNb 18-10 austenitic stainless steels that exposed for long durations of time in acidic solutions were measured by elemental analysis, while their respective surfaces were analyzed using photographs.

1. Introduction

Stainless steels are iron alloys that have of thin, transparent and durable chrome oxide passivation layers. The stability of the passive film and the corrosion resistance of the steel increase with increasing chrome content in the alloy. Although the costs of the stainless steel are higher than those with similar mechanical characteristics, the primary justification for its common usage is improved corrosion resistance. Stainless steels have a large range of applications. Over one-third of produced stainless steels are used in structural applications for chemistry and power engineering industries. These applications include nuclear reactor canals, heat converters, tubes that are used in oil industries, chemistry applications, paper industries' components, and as, the pieces of boilers and furnaces that are used in nuclear reactors [1–7].

Many studies have investigated the corrosion behaviors of 316 austenitic stainless steel. Pardo et al. investigated the effect of Cu and Sn on the pitting corrosion resistance of 304 and 316 stainless steels in a chloride media. These steels were subjected to static potential and electrochemical cyclic polarization measurements in a 3.5% NaCl solution, and the following results were obtained: when copper was added to the structure, it improved nucleation and inhibited corrosion pit growth, while in contrast, the incorporation of tin hindered nucleation and enhanced the pit growth rate [8].

Ilevbare and Burstein and Pardo et al. investigated the effect of incorporated Mo, Mn and chromate ions on the pitting corrosion resistance of 304 and 316 stainless steels. According to this study, ions obstruct the growth pits and strengthen the steel [7–10].

In this study, the corrosion resistance of G-X CrNiMoNb 18-10 austenitic stainless steel which has not been extensively studied was investigated by potentiodynamic polarization curves and the weight loss method in acidic solutions. Furthermore, the hardness, elemental composition and surface morphology of G-X CrNiMoNb 18-10 steel that exposed to corrosive media for long periods of time were analyzed.

2. Materials and methods

2.1. Materials

Austenitic stainless steel, whose standard composition is summarized in Table 1, was used in all experiments. This steel is symbolized with G-X CrNiMoNb 18-10, has a standard number of 1.4580, and AISI number of 316 Cb. Chemical composition is given in Table 2. The values given in Table 2 are compatible with the standards.

The G-X CrNiMoNb 18-10 austenitic stainless steel experimental specimens were quenched in two steps. In the first step, the specimens were heated to a temperature between 1050 and 1150 °C and were immediately cooled in oil. In the second step, the steel specimens were heated to a temperature between 500 and 600 °C, and again cooled in oil.

2.2. Weight loss method

G-X CrNiMoNb 18-10 austenitic stainless steel 5 cm × 2 cm × 0.3 cm plates were used to determine the corrosion rates using the weight loss method. The surfaces of the plates were cleaned by a chemical process, including a $3HNO_3:1H_2SO_4:1H_2O$ mixed solution, followed by pure water and CCl_4. The cleaned specimens were held in a furnace to a fixed mass. Masses of the fixed mass specimens were determined and recorded. The specimens were immersed in 3 M H_2SO_4, 3 M HCl, and 3 M H_2SO_4 + 3 M HCl (1:1) mixed solutions. Two specimens were taken from each solution at specified times (10, 20, 30, 40, 50, 60, 70, 80, 90, 100, 110, and 120 days). The stainless steel

---

[*] Corresponding authors. Tel.: +90 262 3032054; fax: +90 262 3032003.
E-mail addresses: merve@kocaeli.edu.tr, szor2001@yahoo.com (S. Zor).

0925-8388/$ – see front matter © 2009 Elsevier B.V. All rights reserved.
doi:10.1016/j.jallcom.2009.02.069

Table 1
Standard composition of experiment specimen (wt.%) (6).

AISI no.	316 Cb
C (%)	$\leq$0.08
Cr (%)	16.5–18.5
Ni (%)	11–14
Mo (%)	2–2.5
Mn (%)	$\leq$2.0
Nb (%)	$\geq 8 \times$ C
Si (%)	$\leq$1.0
P (%)	$\leq$0.045
S (%)	$\leq$0.03

specimens were taken from solutions, held in 5% citric acid (pH 4.5) for 2 h, and then rinsed with pure water. These specimens were later dried again at 110 °C in a furnace and weighed. Using this process, weight losses were determined and corrosion rates were calculated using the following formula:

$$\text{corrosion rate} = \frac{\text{weight loss}}{\text{surface area of metal} \times \text{time}} \tag{2.1}$$

2.3. Electrochemical method

Electrochemical measurements were made by PAR 263 A, potentiostat/galvanostat. In the electrochemical measurements, platinum was used as the counter electrode, saturated calomel electrode (SCE), as the reference electrode, and G-X CrNiMoNb 18-10 austenitic stainless steel as the working electrode. The surfaces of the working electrode were covered with polyester, except for the parts connected to the solutions. Before measuring, the surface of the working electrode was polished to a mirror finish with a polishing device (METKON GRIPO 2V) using, 800 and 1200 mesh sandpaper. Polarization curves were obtained between −1.00 and +1.00 V at a 1 mV/s scan rate. During the measurement, the solutions were mixed with a magnetic mixer.

All the above experiments were carried out using freshly polished specimens in aerated solutions.

2.4. Hardness test

As shown in Section 2.2 the cleaned specimen plates were immersed in 3 M H_2SO_4, 3 M HCl, and 3 M H_2SO_4 + 3 M HCl (1:1) solutions. Plates were taken at specified times (0, 30, 60, 90, and 120 days), cleaned, and then prepared for the hardness test. The hardness of each prepared plate was determined with a BROOKS Model MAT 10/250 machine using the Rockwell B hardness method.

2.5. Surface analysis

The surfaces of the G-X CrNiMoNb 18-10 austenitic stainless steel plates that were exposed to acidic solutions (3 M H_2SO_4, 3 M HCl, and 3 M H_2SO_4 + 3 M HCl (1:1)) for (0 and 120 days) were investigated by digital photos.

2.6. Elemental analysis

Elemental analysis of samples corroded in acidic solutions was made by TUBITAK (The Scientific and Technological Council of Turkey).

3. Discussion and results

3.1. Weight loss test results

The variance of the corrosion rate as a function of time for G-X CrNiMoNb 18-10 austenitic stainless steel in 3 M H_2SO_4, 3 M HCl, and 3 M H_2SO_4 + 3 M HCl (1:1) solutions is summarized in Fig. 1.

Table 2
Chemical composition of experiment specimen (wt.%).

AISI no.	316 Cb
C (%)	0.077
Cr (%)	16.74
Ni (%)	11.52
Mo (%)	2.173
Mn (%)	1.112
Nb (%)	0.855
Si (%)	0.702
P (%)	0.029
S (%)	0.013

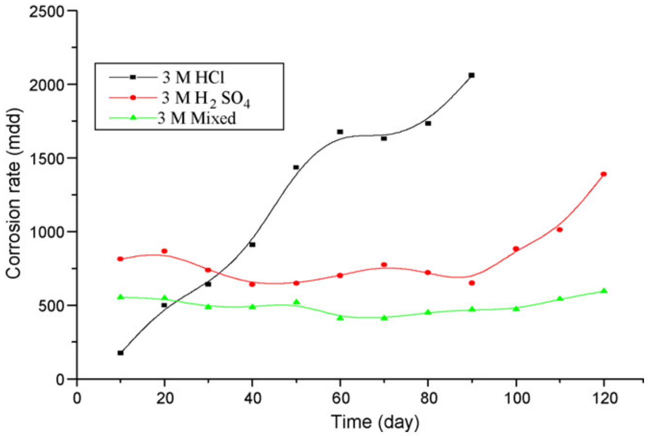

Fig. 1. Varying of corrosion rate according to time for G-X CrNiMoNb 18-10 austenitic stainless steel in 3 M H_2SO_4, 3 M HCl vs. 3 M H_2SO_4 + 3 M HCl (1:1).

According to Fig. 1, the corrosion rates of G-X CrNiMoNb 18-10 austenitic stainless steels in a 3 M HCl solution was observed to increasing, while the steels in other solutions indicated no clear increased corrosion through the protective oxide passivation. Corrosion rates of specimens immersed in a 3 M HCl solution were observed to increase by approximately 11 times, reaching 2060 mdd at the end of 90 days. While the corrosion rates of plates in the 3 M HCl solution were observed to increase for the first 20 days, the rates oscillate up to 90 days due to the cyclical protective oxide layer formation and degradation on the metal surface. After 90 days, the corrosion rates increased due to a breakdown of the protective oxide layer, ultimately reaching 1379 mdd at the end of 120 days. The corrosion rate of G-X CrNiMoNb 18-10 austenitic stainless steel in a mixed solution became constant at the end of 70 days due to the formation of a protective oxide layer. The corrosion rates were observed to increase from 70 to 120 days due to the breaking down of the protective oxide layer on the metal surface. The corrosion rates of austenitic stainless steel in a 3 M HCl solution were observed to be the greatest due to Cl^- ions, followed by 3 M H_2SO_4 and 3 M H_2SO_4 + 3 M HCl (1:1) acidic solutions, respectively (Fig. 1).

3.2. Electrochemical method results

Potentiodynamic polarization curves of G-X CrNiMoNb 18-10 austenitic stainless steel in HCl, H_2SO_4 and H_2SO_4 + HCl (1:1) acidic solutions with different concentrations (0.1, 1, 2, and 3 M) are given in Figs. 2–4.

As shown in the polarization curves in Fig. 2, increasing the acid concentration of austenitic stainless steel HCl immersion solution was observed to increase the corrosion current density from 38.19 $\mu A/cm^2$ (0.1 M HCl) to 4505 $\mu A/cm^2$ (3 M HCl). In this case, Cl^- ions penetrate into the metal surface and increase the concentration of the metal. This effect is also increased with increasing chloride concentration. Furthermore, passivity was not observed for specimens immersed in HCl solutions, but was seen for H_2SO_4 and HCl + H_2SO_4 (1:1) solutions, since Cl^- ions obstruct the oxide at the metal surface (Fig. 2 compared to Figs. 3 and 4). The corrosion potential increases as a function of HCl concentration, which is shown as more negative values.

Fig. 3 depicts the polarization curves of G-X CrNiMoNb 18-10 austenitic stainless steel in 0.1, 1, 2, and 3 M H_2SO_4 solutions. Passivity was observed in all of these curves due to the occurrence of oxide on the metal surfaces. The cathodic reactions in the acidic solutions are hydrogen reductions. The full passivity poten-

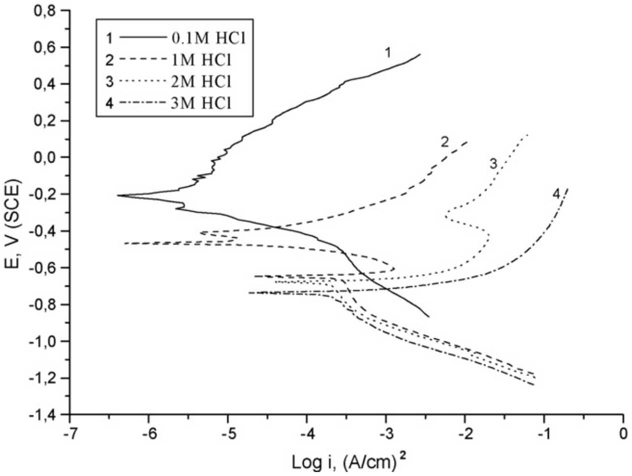

Fig. 2. Potantiodynamic polarization curves of G-X CrNiMoNb 18-10 austenitic stainless steel in HCl.

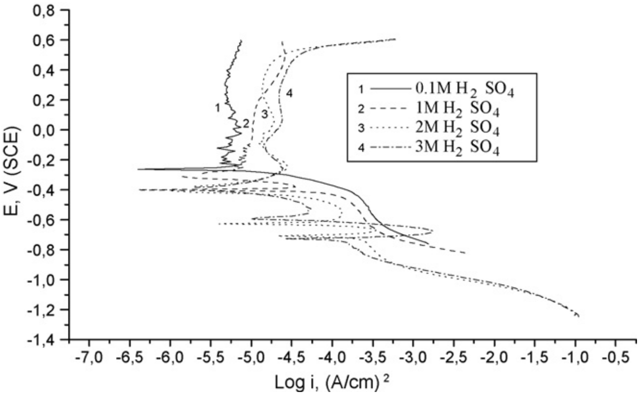

Fig. 3. Potantiodynamic polarization curves of G-X CrNiMoNb 18-10 austenitic stainless steel in H_2SO_4.

tial region was observed to be −0.22–0.55 V in 0.1 and 1 M H_2SO_4, −0.25–0.52 V in 2 M H_2SO_4 and −0.26–0.5 V in 3 M H_2SO_4. The full passivity current density was observed to be 4.90 μA/cm^2 in 0.1 M H_2SO_4, 11.75 μA/cm^2 in 1 M H_2SO_4, 15.85 μA/cm^2 in 2 M H_2SO_4, and 23.44 μA/cm^2 in 3 M H_2SO_4. The full passivity potential region and potential of breaking passivity decrease with increasing H_2SO_4 concentration. The full passivity current density increases with increasing acid concentration.

Fig. 4 depicts the polarization curves of G-X CrNiMoNb 18-10 austenitic stainless steel in HCl + H_2SO_4 (1:1) solutions. Full passivation is performed in 1, 2, and 3 M HCl + H_2SO_4 (1:1) mixing solutions. The flade potential at all concentrations is similar. The full passivity potential region decreases with increasing acid concentration, while the full passivity current density increases with increasing acid concentration.

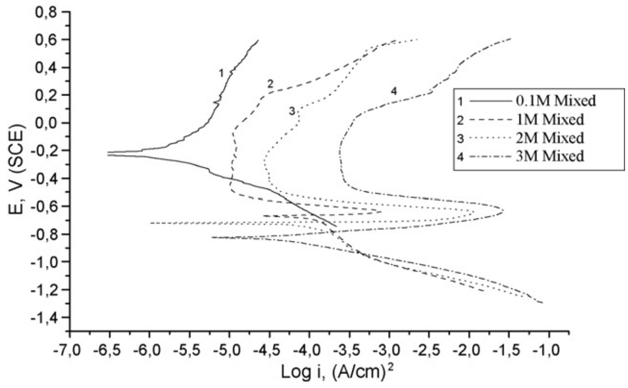

Fig. 4. Potantiodynamic polarization curves of G-X CrNiMoNb 18-10 austenitic stainless steel in HCl + H_2SO_4 (1:1) mixed solutions.

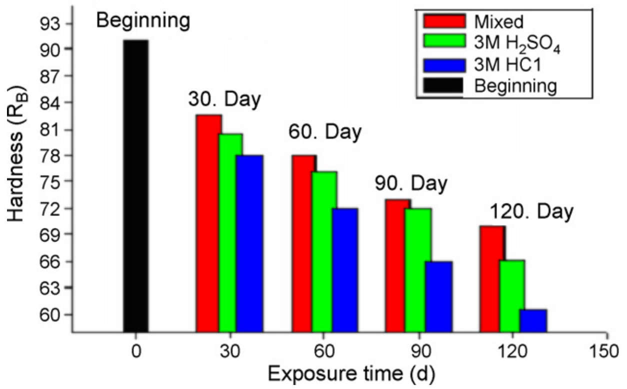

Fig. 5. Varying of G-X CrNiMoNb 18-10 austenitic stainless steel hardness values (R_B) according to exposure time in different acidic solutions.

3.3. Hardness test

The hardnesses of G-X CrNiMoNb 18-10 austenitic stainless steel plates treated with HCl, H_2SO_4, and H_2SO_4 + HCl (1:1) acidic solutions for various durations of time were measured using the Rockwell B hardness method. The hardness was measured from five different points on every surface and averaged to calculate hardness. Fig. 5 depicts the variation of specimen hardness as a function as holding time in the aforementioned solutions.

The hardnesses of the specimens at the beginning were 91 R_B. This value decreased as a function of increased immersion time in the corrosive media. The lowest hardnesses were obtained for specimens immersed in the 3 M HCl solution, while the highest were obtained for those immersed in the 3 M H_2SO_4 + 3 M HCl (1:1) solution. In this manner, hardness and mechanical strength decrease when the corrosion effects increase.

3.4. Surface analysis

Fig. 6 depicts photographs of the G-X CrNiMoNb 18-10 austenitic stainless steel specimens immersed in different acidic solutions for 10 and 120 days. The metal surfaces exposed to any acidic solutions were not appreciably abraded at the end of 10 days, while after 120 days, the surfaces were observed have increased corrosion pitting. Holes and pitting on the metal surfaces were observed for specimens immersed in 3 M HCl solutions due to the corrosive effect of Cl$^-$ ions. The most corrosive effect was caused by HCl solutions.

3.5. Elemental analysis

G-X CrNiMoNb 18-10 austenitic stainless steel specimens exposed for 120 days in acidic solutions were elementally analyzed. According to the analyses, the chrome content of un-immersed specimens was 16.74, while specimens immersed in 3 M HCl, 3 M H_2SO_4, and 3 M H_2SO_4 + 3 M HCl (1:1) solutions were 16.53, 16.58, and 16.61, respectively, after 120 days (Table 3). This observed decrease in chrome content demonstrates that pitting corrosion occurs preferentially on grain boundaries. The content of nickel, providing corrosion resistance beside chrome, also decreased in all acidic solutions. The content of molybdenum and manganese added to increase localized corrosion resistance in chlorinated solutions also decreased. The content of other elements decreased too, as the

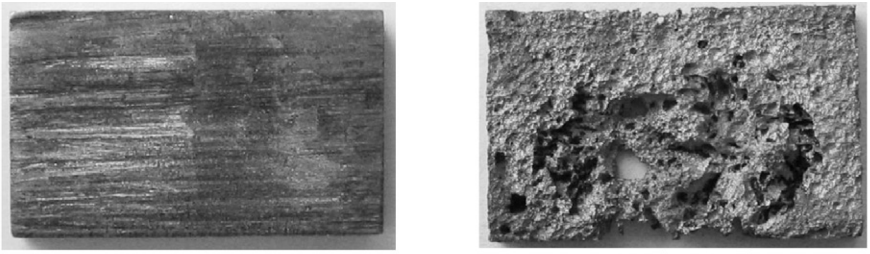

10. day HCl 120. day HCl

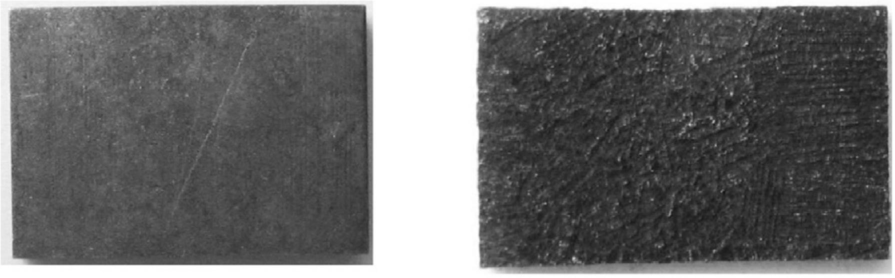

10. day H_2SO_4 120. day H_2SO_4

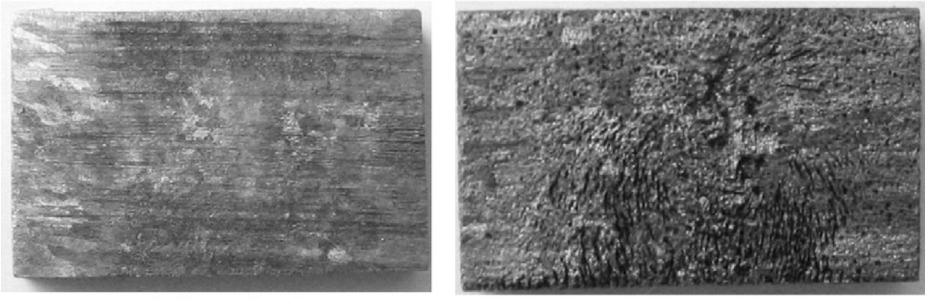

10. day mixed 120. day mixed

Fig. 6. General photographs of G-X CrNiMoNb 18-10 austenitic stainless steel in different acidic solutions at 10 and 120 days.

Table 3
Elemental analysis results of samples corroded in acidic solutions (wt.%).

	Cr (%)	Ni (%)	Mo (%)	Mn (%)	Nb (%)	Si (%)	P (%)	S (%)
In HCl	16.53	11.24	2.089	1.012	0.836	0.673	0.024	0.011
In H_2SO_4	16.58	11.34	2.15	1.090	0.838	0.682	0.025	0.012
In acid mixed	16.61	11.48	2.162	1.102	0.840	0.693	0.025	0.012

G-X CrNiMoNb 18-10 austenitic stainless steel stayed for a long time in corrosive environment (Table 3).

4. Conclusions

- The corrosion rate of G-X CrNiMoNb 18-10 austenitic stainless steel was increased according to the weight loss method. The greatest increase was observed in 3 M HCl solution.
- Full passivity in HCl solutions was not observed in the potentiodynamic polarization measurements.
- According to hardness tests, the hardness of G-X CrNiMoNb 18-10 austenitic stainless steel decreases while corrosion effects increase.
- The occurrence of pitting corrosion on metal surfaces was determined from photographic films.
- A decrease in chrome and other elements content was observed from elemental analysis results.

References

[1] J.R. Davis, Metals Handbook, Second edition, Davis & Associates, ASM, 1998, p. 362.
[2] Z. Szklarska-Smialowska, Corrosion 27 (1971) 223.
[3] A.J. Sedriks, Corrosion of Stainless Steels, John Wiley and Sons, New York, 1979.
[4] U. Kamachi Mudali, S. Ningshen, A.K. Tyagi, R.K. Dayal, Mater. Sci. Forum 318–320 (1999) 495.
[5] B. Mazza, P. Pedeferri, D. Sinigaglia, A. Cigada, G. Fumagalli, G. Re, Corros. Sci. 19 (1979) 907.
[6] A. Barbucci, M. Delucchi, M. Panizza, M. Sacco, G. Cerisola, J. Alloys Compd. 317–318 (2001) 607.
[7] G.O. Ilevbare, G.T. Burstein, Corros. Sci. 45 (2003) 1545.
[8] A. Pardo, M.C. Merino, M. Carboneras, A.E. Coyand, R. Arrabal, Corros. Sci. 49 (2007) 510.
[9] A. Pardo, M.C. Merino, A.E. Coy, F.R. Viejo, Corros. Sci. 50 (2008) 1796.
[10] A. Pardo, M.C. Merino, A.E. Coy, F.R. Viejo, R. Arrabal, E. Mathykina, Corros. Sci. 50 (2008) 780.